Renewable Energy 132 (2019) 439–454

Contents lists available at ScienceDirect

Renewable Energy

journal homepage: www.elsevier.com/locate/renene

Techno-economic optimisation of offshore wind farms based on life cycle cost analysis on the UK

Varvara Mytilinou [a,*], Athanasios J. Kolios [b]

[a] Renewable Energy Marine Structures Centre for Doctoral Training, Cranfield University, Cranfield, MK43 0AL Bedfordshire, United Kingdom
[b] Department of Naval Architecture, Ocean & Marine Engineering, University of Strathclyde, Henry Dyer Building, 100 Montrose Street, Glasgow G4 0LZ, United Kingdom

ARTICLE INFO

Article history:
Received 14 April 2018
Received in revised form 14 July 2018
Accepted 30 July 2018
Available online 3 August 2018

Keywords:
Life Cycle Cost
NSGA II
Multi-objective optimisation
Round 3
UK
Sensitivity analysis

ABSTRACT

In order to reduce the cost of energy per MWh in wind energy sector and support investment decisions, an optimisation methodology is developed and applied on Round 3 offshore zones, which are specific sites released by the Crown Estate for offshore wind farm deployments, and for each zone individually in the UK. The 8-objective optimisation problem includes five techno-economic Life Cycle Cost factors that are directly linked to the physical aspects of each location, where three different wind farm layouts and four types of turbines are considered. Optimal trade-offs are revealed by using NSGA II and sensitivity analysis is conducted for deeper insight for both industrial and policy-making purposes. Four optimum solutions were discovered in the range between £1.6 and £1.8 billion; the areas of Seagreen Alpha, East Anglia One and Hornsea Project One. The highly complex nature of the decision variables and their interdependencies were revealed, where the combinations of site-layout and site-turbine size captured above 20% of total Sobol indices in total cost. The proposed framework could also be applied to other sectors in order to increase investment confidence.

1. Introduction

According to the 20-20-20 target on reducing carbon emissions and the Climate Conference in Paris (COP 21) on keeping the global warming temperature below 2 °C, it is important to contribute to the Renewable Energy (RE) investment growth in the UK by making the investments more attractive, information-rich and less risky [1]. The UK technology roadmap highlights that the offshore wind costs need to be reduced to £100 per MWh by 2020 and greater confidence over financial motivations is required [2].

Offshore wind managed to reach 24% of the total installed power in Europe in 2015 compared to the 13% share the previous year [3]. Currently, 1716 offshore turbines are deployed in 32 offshore operational projects of an overall capacity of 6713.520 MW in the UK [4]. However, significant price increases in the overall cost of turbines, their operational and maintenance costs etc. have a direct impact on large-scale wind projects. The location of a wind farm and the type of support structure have great impacts on the overall costs [5–7].

Ensuring a long-term and profitable investment plan for investors and developers can be challenging. In many cases, both pre-consent and post-consent delays cause inconveniences. Considerable actions are mandated, on top of the development plans, for minimising investment, developing the supply chain, securing consents, ensuring economic grid investment and connection, and accessing finance [2,8]. Overall, appropriate studies should be conducted at the early development stages of the project in order to avoid disruptions and minimise the investment risk. A very important decision that appears when starting a new investment is the selection of a suitable offshore location (zone and site) and always requires extended effort from developers. The location of a wind farm and the type of support structure have great impacts on the installation costs. The most important costs in an offshore wind farm can be found in Ref. [9].

In Ref. [10], a study was conducted in order to discuss and compare the results among three state-of-the-art optimisation evolutionary and genetic algorithms (NSGA II, NSGA III and SPEA 2) and then applied to a real-world case of the wind energy sector. A set of optimum locations for a wind farm are suggested by considering only round 3 zones, which are specific sites released by

* Corresponding author.
E-mail addresses: v.mytilinou@cranfield.ac.uk (V. Mytilinou), athanasios.kolios@strath.ac.uk (A.J. Kolios).

https://doi.org/10.1016/j.renene.2018.07.146

Nomenclature

A	Area of the wind turbine (m^2)
C_p	Power coefficient
$C_{P\&C}$	Predevelopment and Consenting cost (£)
$C_{P\&A}$	Production and Acquisition cost (£)
$C_{I\&C}$	Installation and Commissioning cost (£)
$C_{O\&M}$	Operation and Maintenance cost (£)
$C_{D\&D}$	Decommissioning and Disposal Cost (£)
CAPEX	Capital Expenditures (£)
LCC	Life Cycle Cost (£)
NWT	Number of turbines
OPEX	Operational expenditure (£)
P_R	Rated power (W)
u	Mean annual wind speed of each specific site (m/s)
TIC	Total Installed Capacity (W)
ρ	Air density (kg/m^3)

the Crown Estate, where the developers can install and deploy offshore wind farms around the UK. The study considered some of the most important techno-economic Life Cycle Cost (LCC) factors that are directly linked to the physical aspects of each wind farm location such as the wind speed, the distance from the construction ports and the water depth. Optimal solutions were discovered by all three algorithms and such outcomes are expected to reveal the benefits of possible extensions of the Round 3 zones in the future of the UK and will help decision makers for their next cost-efficient investment decision.

The aim of this paper is to establish a methodology for the decision-making process at the initial stages of a wind farm investment of Round 3 zones in the UK that reveals the optimum offshore locations by considering a model that combines techno-economic factors of the LCC analysis, layout selection and location-based constraints. The revealed optimum solutions per zone and a reference selection of zones will offer flexibility at the cost budget assignment phase of the wind farm development and is aligned with the reduction of the cost of energy at less than £100 per MWh. It is also expected that the differences among three suggested wind farm layouts will be explored by considering the conflicting nature of the cost elements. The outcomes will provide further insight into wind energy sector for future investments.

The contribution of this work follows. First, as illustrated in Fig. 1, it proves the effectiveness of the developed framework that links the economic modelling of the LCC analysis to an optimisation method, where the solutions comprise of wind farm layouts, offshore Round 3 locations in the UK, number of turbines and turbine size. The interplay between CAPEX and OPEX will be revealed through multi-objective optimisation and quantified based on each decision variable through sensitivity analysis. This study assists project developers and researchers at the first stages of the development of a wind farm in order to select an optimum, economically efficient and viable option.

The remaining structure of the paper consists of a literature review on LCC analysis, turbine layout optimisation, wind farm location selection and cost related frameworks in the offshore wind energy sector. Next, the methodology of the present study will follow. The non-dominated results for all zones and each zone individually will be analysed and discussed. Future avenues will be drawn in the conclusions.

2. Literature review

2.1. Offshore wind farm location selection

The UK has released 3 Rounds of offshore wind farm sites for leasing. The 3 Round divisions appeared because of the administrative licensing process adopted by the UK and reflect the development of offshore power collection and transmission systems. In Round 1, the developments were small (up to 90 MW) and with up to thirty turbines each and near the shore (less than 30 km away from the shore). Round 2 sites were released later and contained larger projects up to 500 MW and a bit further away from the shore (up to 90 km). Finally, Round 3 is currently undergoing planned installations up to 1000 MW and 300 km distance from the shore [11]. When the Crown Estate released the new Round 3 offshore wind site leases, they provided nine new considerably larger zones that include up to 32 GW of power capacity. The new leases encourage larger scale investments and consequently bigger wind turbines. The new zones include locations further away from the shore and in deeper waters which could be more challenging [2,8,12–14].

The Round 3 zones are the following; Moray Firth, Firth of Forth, Dogger Bank, Hornsea, East Anglia (Norfolk Bank), Rampion (Hastings), Navitus Bay (West Isle of Wight), Atlantic Array (Bristol Channel) and Irish Sea (Celtic Array). Every zone consists of various sites and extensions. In this study, the five first zones in the North Sea are investigated. The selected zones provided a group of sites. These groups were selected as a reference case in order to prove the present methodology that provides results for both overall and individual zones.

Each location faces similar challenges; deep waters or high distances from the shore, etc. For example, Dogger Bank offers some advantages because of its shallow waters and high wind speed (above 10 m/s). It also offers economies of scale. However, it faces marine environmental issues and long distance from the shore and thus the ports, which has a costly impact [15]. The Round 3 offshore zones and sites are shown in the following Fig. 2.

In literature, only a few location-selection-focused studies can be found but the findings and the formulation of the problems provided follow a different direction. Goal programming was used in Ref. [16] in order to obtain the optimum offshore location for a wind farm installation. The study involves round 3 locations in the UK and discusses its flexibility to combine decision-making. The work shows the energy production, costs and multi-criteria nature of the problem while considering environmental, social, technical and economic aspects.

A study on offshore locations for a RE platform by using multiple criteria and Geographical Information Systems (GIS) is provided in Ref. [17]. Issues around offshore RE platforms have been reviewed and a combination of criteria has been selected for the Atlantic facing shores in Europe. Potential risks and trade-offs between designing costs and energy production were discovered. Factors such as the lack of construction ports that results in under-exploited sites, access problems and weather window conditions, even during the summer months were provided. The study is mostly focused on environmental, geographical and weather issues.

Similarly, a study for the optimum selection of wind turbines was conducted in Ref. [18] by considering cost-effective criteria and especially the cost of energy and the local wind conditions. The study demonstrates the need for a framework to deal with such challenging problems where a decision is necessary. In Ref. [19], a selection method of the optimum access point for offshore wind farms in China is suggested by using multi-objective optimisation and a comprehensive weight decision-making method, Analytic

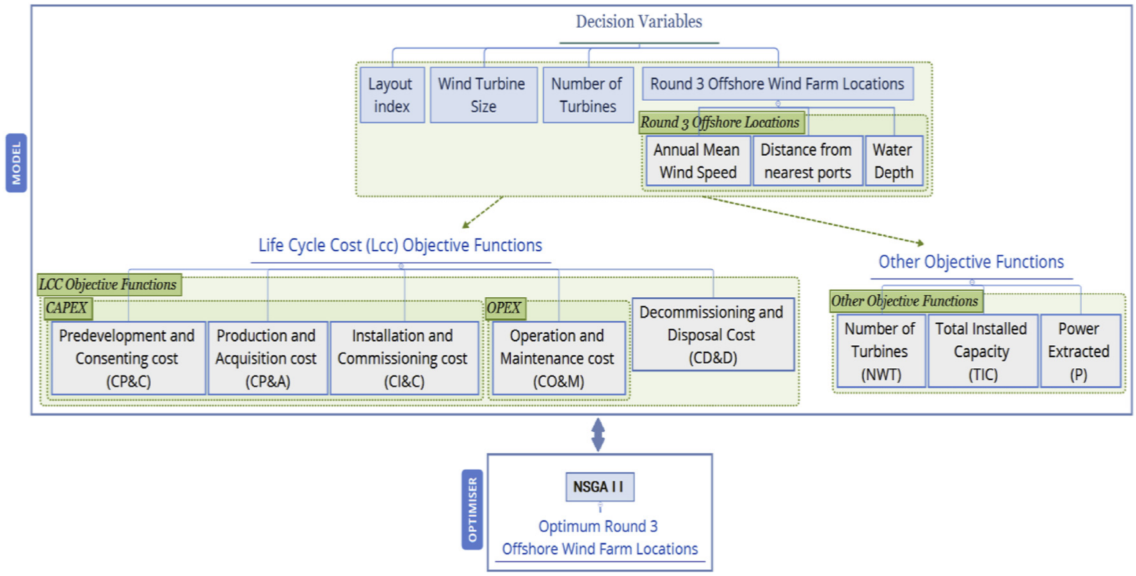

Fig. 1. Framework outline.

Hierarchy Process (AHP). The study selects the optimum access point in a power grid for an offshore wind farm which is integrated into the onshore power system. Although similar methods were employed, none of these studies shows a focus on the location selection for renewable installation employing life cycle cost factors.

2.2. Life cycle cost analysis

The LCC analysis can evaluate costs and suggest cost reductions throughout a project's whole life. The outcome of the analysis can provide deeper insight into an investment and can impact on direct decision making from the initial stages of a new project [20]. LCC analysis gains more ground over the years because of the larger scale in wind projects. For example, the advantages and disadvantages of the transition to offshore wind and a LCC model of an offshore wind development were proposed in Ref. [21]. However, the present study mainly focuses on a simplified model and especially the operation and maintenance stage of the LCC analysis and it is suggested that there can be a further full-scale LCC framework in the future. More studies can be found in Refs. [22–28].

Calculating the LCC of a wind farm and especially an offshore wind project can be very challenging. It involves many cost phases from the predevelopment to the decommissioning phase, and there is not any common universal reference point for wind projects. In Ref. [29], a parametric whole life cost framework for an offshore wind farm and a cost breakdown structure is presented and analysed. LCC analysis is essential for the insurers, wind farm operators and investors in order to ensure a cost-efficient long and profitable investment plan to produce power. In Ref. [29] the LCC analysis was divided into five stages of the wind project as a guideline; the predevelopment and consenting ($C_{P\&C}$), production and acquisition ($C_{P\&A}$), installation and commissioning ($C_{I\&C}$), operation and maintenance ($C_{O\&M}$), and decommissioning and disposal ($C_{D\&D}$) stage.

There are limited studies that combine the concept of LCC analysis with MOO. There are no studies that consider objectives based on economic figures in order to select the optimum Round 3 offshore location in the UK. In fact, for the selection of the location, there is very limited work accessible and with a small amount of focused and related criteria on this topic. The present study focuses on all five components of the LCC costs in Ref. [29]. It also considers three different cases of turbine layouts based on the theory behind the positioning and an extreme case, in order to find the optimum offshore location for wind farm projects. This study also provides optimum location solutions both in the overall Round 3 zones and individual location solutions per Round 3 zone.

2.3. Genetic algorithms

NSGA stands for Non-dominated Sorting Genetic Algorithm and it is also a MOO algorithm and an Evolutionary Multi-criterion Optimisation (EMO). Currently, there are three versions of the code; NSGA, NSGAII and NSGAIII [30]. This research employs the NSGA II algorithm because of its suitability for this type of MOO problems with many objectives as discussed in Ref. [10].

The design of a new evolutionary based optimisation algorithm is proposed in Ref. [31], in order to optimise the layout of turbines in a wind farm. The shape of the wind farm, a range of costs and orography were included. Five different types of optimisation algorithms were used in Ref. [32] in order to optimise the layout of a wind farm. Higher quality solutions are expected to be discovered by using algorithms with stochastic elements. Combining genetic algorithms with heuristics was more effective and faster than using one of them.

In Ref. [33], the authors optimised the layout of a wind farm (micro-siting optimisation: choosing the type and location of wind turbines) by considering continuous space and by using particle swarm optimisation techniques. A special local search scheme was also introduced in the optimisation algorithm to successfully speed up the process. Finally, evolutionary algorithms are applied to a wind farm optimisation problem in Ref. [34]. The configuration of the layout of the turbines is optimised based on a cost model. The suitability of the suggested evolutionary techniques is proven in the study. More can be found in Refs. [35–37].

2.4. Wind farm layouts

Layout optimisation is a significantly complex problem and is governed by many trade-offs. The problem is usually solved by

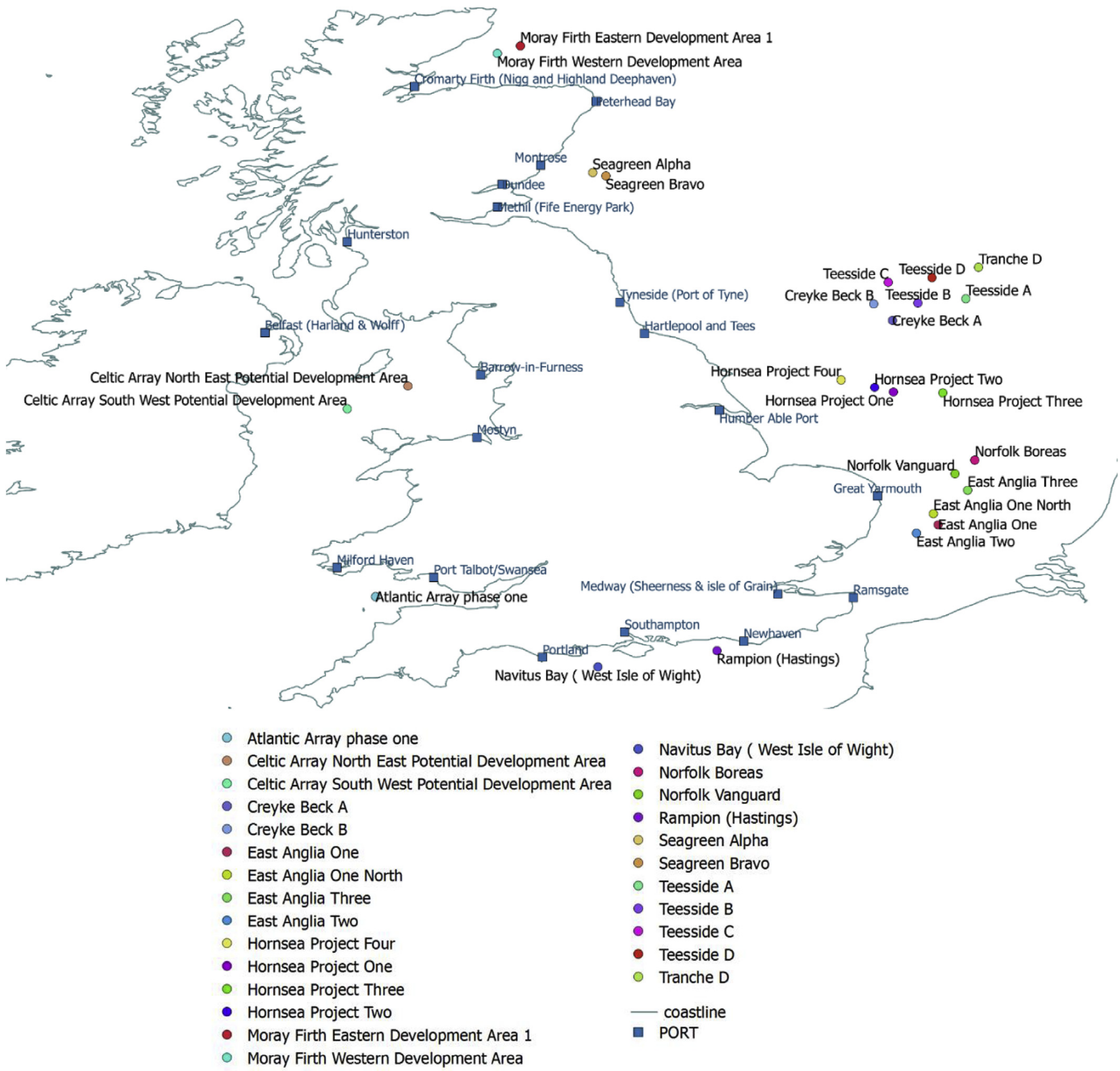

Fig. 2. Round 3 offshore location around the UK by using QGIS.

using layout optimisation processes that position the turbines accordingly in order to reduce/minimise the wake effect and, at the same time, to increase/maximise the produced power [38,39]. Wind turbines are usually placed in groups in order to efficiently transform wind energy to electricity and reduce installation and maintenance costs at the same time. However, although cost reduces by grouping turbines, the power extracted from them is considerably decreased. Turbulence or wake effect created by each turbine can affect the ones that are at their wake and thus many studies aim to reduce these wake effects in order to maximise the produced power, especially at large scale offshore farms. In order to achieve the optimum positioning, identical rows and large distances between turbines or irregular positioning yield better power production and profit [3,39]. When optimising the layout, minimising the distance between turbines reduces the cabling costs but increases the wake effect, which minimises energy generation [40].

The problem with multiple wake effects in a wind farm is the wind speed deficit, which depends on the nearest turbines. At a large scale, though, the phenomenon is not fully comprehended. Many studies in the aerodynamic sector are focused on this effect and their results show disagreements among the studies and real large-scale wind farms, where the wake effect is the most relevant and appears to have a heavy impact [39,41]. The methodology behind layouts is the basic theory of the rule of thumb. According to the rule, the prevailing theory, wind turbines are usually placed 5–9 times the rotor diameter at the dominant-for-the-location wind speed direction and 3–5 times the diameter vertical to the previous mentioned dominant wind speed as shown in Fig. 3. Other studies use even ten times the diameter between the rows and seven times along the rows.

The number and the size of the turbines to be installed are determined by the size of the investment and also depend on each other (number of turbines vs turbine size). Bigger turbine size is usually preferred because the cost and the energy production are usually proportional to its nominal power. Therefore, the net profit from each turbine is also proportional to its nominal power. However, sometimes even if it is more sensible to employ large-scale turbines, the price of smaller turbines might be considerably lower [39].

The first study to consider the layout optimisation was [42]. A wind farm site modelled with 100 possible squares and their centres as points for the position of the turbines in order to ensure the validity of the Jensen model where each square side is five times the diameter of the turbine (5D) [43,44]. In Ref. [45], a multi-objective genetic algorithm is employed on an island in the Aegean sea. The maximisation of the energy extracted and the minimisation of the cost is provided. The study assumes the wind direction stable and the wind speed constant. The minimum space between turbines is considered as eight times the diameter of the turbine (8D) in the prevailing wind direction and only two times the diameter at the crosswind direction (2D). The Pareto Front (PF) solutions of this study provided the optimum configurations, the total power produced, cost and number of turbines. Although the cost and the number of turbines are optimised, no economic model or LCC was presented. The study focuses mostly on the wake effect.

The layout optimisation problem is addressed throughout the literature in many scientific publications. However, the studies do not consider the construction and logistics in the calculations. To the best of the authors' knowledge, in literature LCC analysis and three different offshore layout cases were never linked before to a MOO formulation in order to conclude to the optimum wind farm location. The offshore wind farm selection is studied by each developer individually and never has a framework appeared in order to guide researchers and decision makers, so as to make informed and low-in-risk decisions.

3. A framework for the optimisation of deployment sites for round 3 wind farms in the UK

The LCC analysis of a project is always challenging. It involves

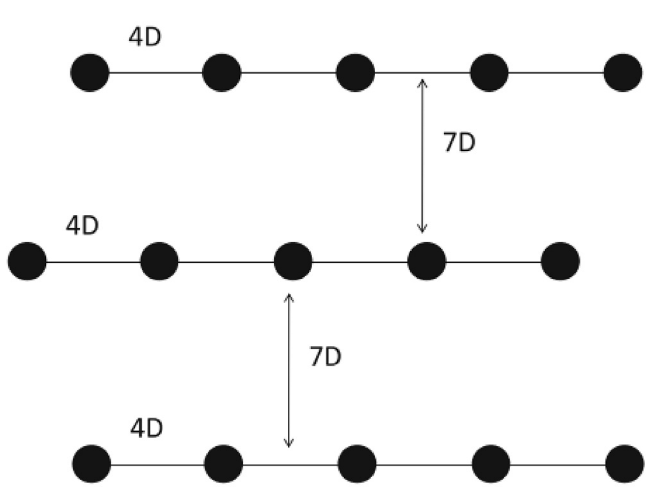

Fig. 3. Wind farm layout as introduced in Ref. [39].

stages from the predevelopment to the decommissioning phase. In Refs. [29,46], a whole LCC formulation is provided and this study integrates these phases into the optimisation problem, as shown in Fig. 4. Assumptions and related data in the modelling of the problem can be found in the following references [26,29,46–50]. Based on the previous references, a new model was developed, so as to be coupled with the optimisation algorithm and drive the optimisation search. The LCC model described in Ref. [29] is used as a guideline in this study and its structure is provided below in detail. The type of foundation that was considered in the LCC model in the present work is the jacket structure.

The LCC, CAPEX and OPEX represent the Life Cycle Cost, Capital expenditure and Operational expenditure, respectively and they are calculated as follows. The individual costs are the following; $C_{P\&C}$ is the Predevelopment and Consenting cost, $C_{P\&A}$ is the Production and Acquisition cost, $C_{I\&C}$ is the Installation and Commissioning cost, $C_{O\&M}$ is the Operation and Maintenance cost, and finally, $C_{D\&D}$ is the Decommissioning and Disposal Cost.

$$LCC = C_{P\&C} + C_{P\&A} + C_{I\&C} + C_{O\&M} + C_{D\&D}$$

$$CAPEX = C_{P\&C} + C_{P\&A} + C_{I\&C}$$

$$OPEX = C_{O\&M}$$

The framework described in this section is suggested in order to assess the effectiveness of the suggested methodology to discover the optimum location from a selection of Round 3 offshore locations in the North Sea, in the UK. Conceptually, the framework comprises of a model and an optimisation algorithm, also shown in Fig. 1. Fig. 5 shows the framework with the extension of a decision making phase and links to the other phases.

The optimisation problem includes eight objectives; five LCC-related objectives, as described in Ref. [29], and three additional objectives. Optimising eight objective functions at the same time, which are conflicting (from the mathematical formulation above), classifies the problem as many-objective and it is considered rather complicated because of the interplay of the objectives, the nature of the variables and the nature of the constraints.

For the selection of the optimum offshore wind farm location, physical aspects of each location, i.e., wind speed, water depth and distance from designated construction ports, are considered. A list of ports was acquired from Refs. [51–53]. The list contains designated, appropriate and sufficient construction ports that are suitable for the installation, manufacturing and maintenance work for wind farms. New ports are agreed to be built for the conveniences of new wind farms. However, this study assumes that the list below contains a selection of currently available ports around the UK.

Table 1 was acquired from Ref. [49], for each offshore location a special profile was created including the coordinates, the distances to the shore and port, annual wind speed and average site water depth. Among various data, Table 1 shows the locations that each of these zones contains. Each location correlates with their specific data used in this problem.

For the distances from the ports calculation, QGIS was used. QGIS is an Open Source licensed Geographic Information System (GIS), which is a part of the Open Source Geospatial Foundation (OSGeo) [51]. These distances were calculated under the assumption that the nearest port to the individual wind farm is a straight line. In this study, the distances represent the route of the ships and impact the overall costs. The real shipping routes were not considered and for this reason, a simplification of the real routes was assumed instead. The straight lines were calculated by using QGIS because of simplicity of the approximation and to demonstrate the proof-of-concept. The estimated metrics were integrated

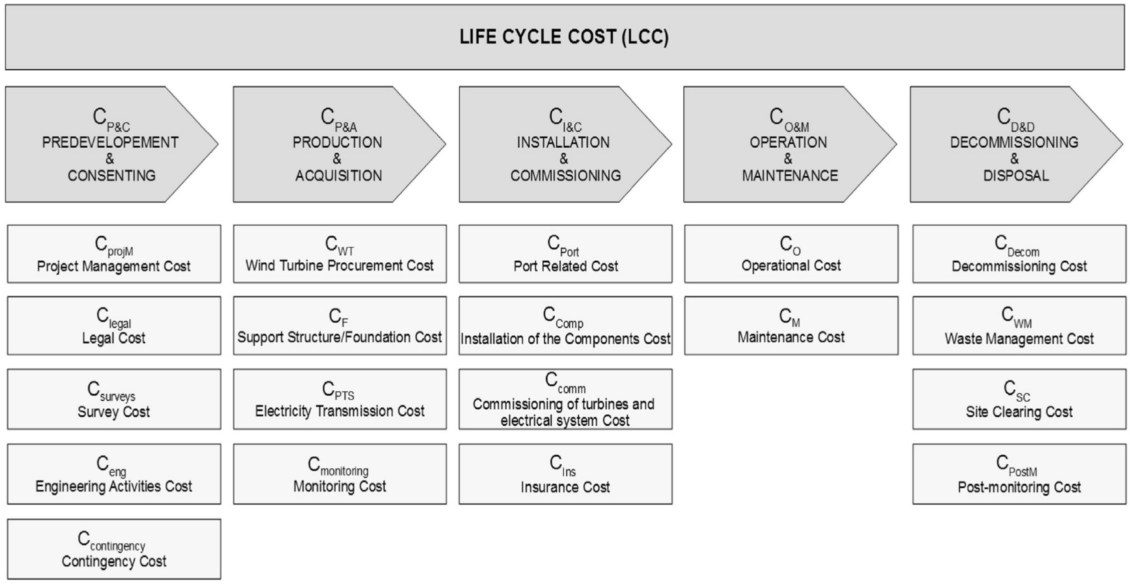

Fig. 4. Life Cycle Cost (LCC) break down [29].

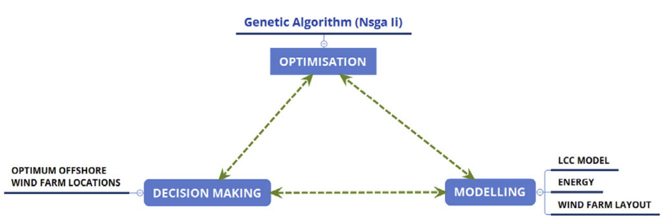

Fig. 5. Framework for the layout and location selection optimisation.

into the configuration settings of the whole LCC.

The lower and upper limits of a theoretical array layout will be compared and contrasted to an extreme case. More specifically, in the lower limit case (3–5 layout), the horizontal and vertical distance between turbines is 3 and 5 times the rotor diameter, respectively. In the upper limit case (5–9 layout), 5 and 9 times the rotor diameter were considered horizontally and vertically. In the extreme case (10–18 layout), the horizontal and vertical distance between turbines is 10 and 18 times the rotor diameter. All cases are depicted in Fig. 6. The present work focuses on the optimisation of offshore wind farm locations considering the maximum wind turbine number that can fit in the selected round 3 locations according to three different layout configuration placements. The wind farm is oriented according to the most optimal wind direction (South West) as investigated and mentioned below. The maximum number of turbines is determined by considering types of reference turbines of 6, 7, 8 and 10 MW, whose specifications are listed in Table 2. The three layout cases are depicted in Fig. 6 and listed in Table 3, where D is the diameter of each turbine. According to the topology capacity and the three layout cases, the calculated maximum number of turbines is listed from Table 5 and Tables 6 and 7(in Appendix A), and all this is integrated into the model.

In Fig. 7, the example of Moray Firth zone (which includes Moray Firth Western Development Area and Moray Firth Eastern Development Area 1) shows the positioning of the turbines considering layouts 1, 2, 3 and turbine sizes.

The wind rose diagrams provided the prevailing wind direction, which sets the layout orientation. All wind farm sites were discovered to have dominant southwestern winds followed by western winds. For that reason, the orientation of the layouts is assumed to be southwestern (as the winds are assumed to blow predominantly from that direction). The wind rose graphs for each offshore site are acquired from Ref. [52].

The QGIS maps of the offshore sites were acquired from the official Crown Estate website [53] for QGIS and AutoCAD. The wind speeds, the wind rose graphs and the coordinates of each location were obtained by FUGRO and 4COffshore [49,52].

The first five objectives of the MOO problem are the costs of the LCC analysis. More specifically, the present model includes the predevelopment and consenting, production and acquisition, installation and commissioning, operation and maintenance and finally decommissioning and disposal costs. All the cost related objectives are minimised.

The last three objectives are the number of turbines (NWT), the power that is extracted (P) from each offshore site and the total installed capacity (TIC), which are minimised, maximised and maximised, respectively. The power extracted is calculated by the specific mean annual wind speed of each location along with the characteristics of each wind turbine both of which are considered inputs (listed in Table 1).

The power extracted in this optimisation model is maximised and it is calculated for each site and each wind turbine respectively from:

$$P = \frac{1}{2} A C p \rho u^3$$

where A represents the area of the wind turbine, Cp is the power coefficient, ρ is the air density and u is the mean annual wind speed of each specific site. The wind speeds used in the calculations were assumed to be the same for each turbine and for each location. This simplification was used in order to demonstrate the effectiveness of the methodology as a proof-of-concept.

The last objective of the model is the TIC, which is calculated by the number of turbines and the rated power of each of them.

Table 1
Round 3 zones & sites and specific data acquired from Ref. [49].

Site Index	Zone	Wind farm site name	Centre Latitude	Centre Longitude	Port	Distance from the port [km]	Annual wind speed [m/s] (at 100 m)	Average Water Depth [m]
0	Moray Firth	Moray Firth Western Development Area	58.097	−3.007	Port of Cromarty	123.6	8.8	44
1	Moray Firth	Moray Firth Eastern Development Area 1	58.188	−2.720	Port of Cromarty	157.1	9.4	44.5
2	Firth of Forth	Seagreen Alpha	56.611	−1.821	Montrose	72.5	9.9	50
3	Firth of Forth	Seagreen Bravo	56.572	−1.658	Montrose	91.1	10	50
4	Dogger Bank	Creyke Beck A	54.769	1.908	Hartlepool and Tess	343.2	10	21.5
5	Dogger Bank	Creyke Beck B	54.977	1.679	Hartlepool and Tess	319.9	10	26.5
6	Dogger Bank	Teesside A	55.039	2.822	Hartlepool and Tess	447.1	10	25.5
7	Dogger Bank	Teesside B	54.989	2.228	Hartlepool and Tess	380.7	10	25.5
8	Hornsea	Hornsea Project One	53.883	1.921	Grimsby	242.3	9.6	30.5
9	Hornsea	Hornsea Project Two	53.940	1.687	Grimsby	217.2	9.7	31.5
10	Hornsea	Hornsea Project Three	53.873	2.537	Grimsby	310.5	9.7	49.5
11	Hornsea	Hornsea Project Four	54.038	1.271	Grimsby	173.9	9.7	44.5
12	East Anglia (Norfolk Bank)	East Anglia One	52.234	2.478	Great Yarmouth	92.7	9.5	35.5
13	East Anglia (Norfolk Bank)	East Anglia One North	52.374	2.421	Great Yarmouth	81.1	9.7	45.5
14	East Anglia (Norfolk Bank)	East Anglia Two	52.128	2.209	Great Yarmouth	74.5	9.4	50
15	East Anglia (Norfolk Bank)	East Anglia Three	52.664	2.846	Great Yarmouth	124.9	9.5	36
16	East Anglia (Norfolk Bank)	Norfolk Boreas	53.040	2.934	Great Yarmouth	143.4	9.5	31.5
17	East Anglia (Norfolk Bank)	Norfolk Vanguard	52.868	2.688	Great Yarmouth	111.4	9.5	32

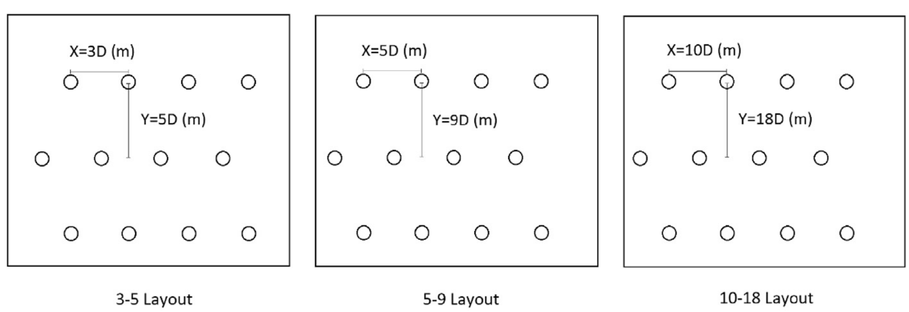

Fig. 6. Demonstrating different layouts, where D corresponds to the diameter of the turbine.

Table 2
Turbine specifications.

Turbine Type Index	Rated power (MW)	Rotor Radius (m)	Hub Height (m)	Total Weight (t)
0	10	95	125	1580
1	8	82	123	965
2	7	77	120	955
3	6	70	100	656

Table 3
Layout specification.

Layout name	X separation	Y separation
3-5 layout	3D	5D
5-9 layout	5D	9D
10-18 layout	10D	18D

$$TIC = P_R \times NWT$$

where P_R represents the rated power and NWT is the number of turbines.

The optimisation problem formulates as follows:

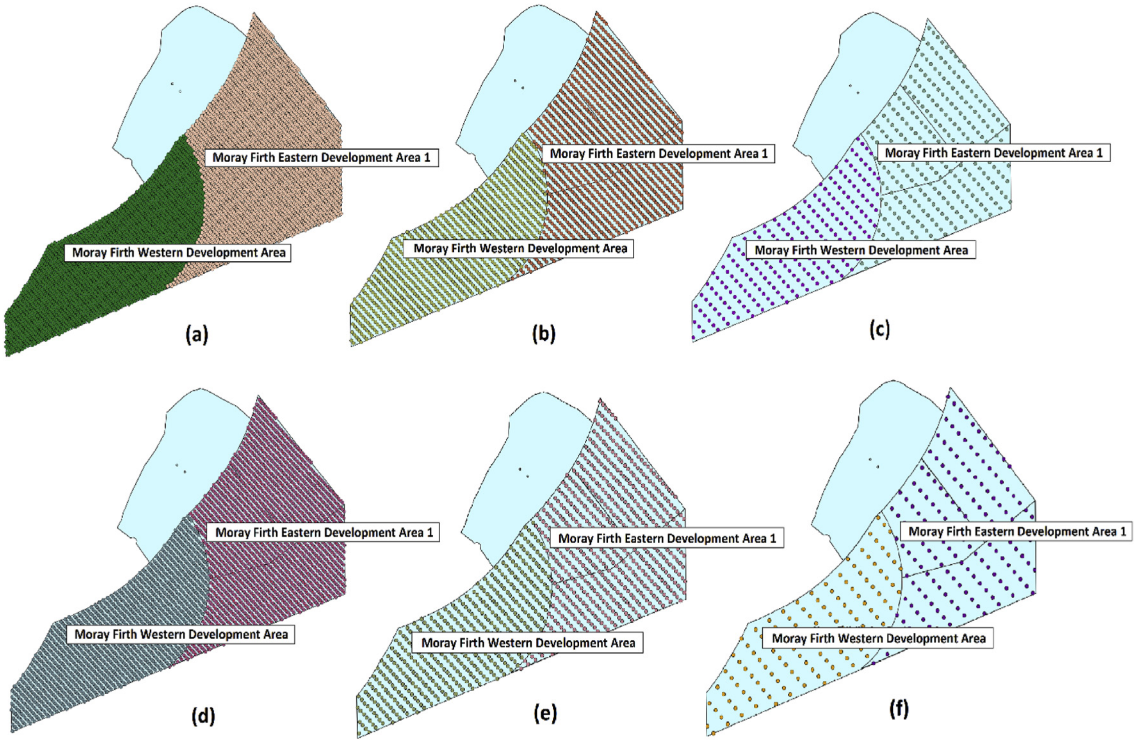

Fig. 7. Moray Firth zone. Maximum number of wind turbines placed according to 3–5 layout, 5–9 layout and 10–18 layout for the case of 10 and 6 MW turbine. In (a) Moray Firth, 6 MW turbines positioned in 3–5 layout, (b) Moray Firth, 6 MW turbines positioned in 5–9 layout, (c) Moray Firth, 6 MW turbines positioned in 10–18 layout, (d) Moray Firth, 10 MW turbines positioned in 3–5 layout, (e) Moray Firth, 10 MW turbines positioned in 5–9 layout, (f) Moray Firth, 10 MW turbines positioned in 10–18 layout.

$$
\begin{array}{ll}
\text{Minimise} & C_{P\&C},\ C_{P\&A},\ C_{I\&C},\ C_{O\&M},\ C_{D\&D},\ \text{NWT},\ (-\text{P}),\ (\text{TIC}) \\
\text{Subject to} & 0 \le \text{site index} \le 20, \\
& 0 \le \text{turbine type index} \le 3 \\
& 1 \le \text{layout index} \le 3 \\
& 0 \le \text{Number of turbines} \le \text{maximum turbine number per site} \\
& TIC \le M\text{aximum capacity of Round 3 sites based on the Crown Estate}
\end{array}
$$

Although the maximum numbers of turbines have been estimated by using QGIS, the maximum capacity allowed per region was also considered, as specified by the Crown Estate in Table 4. Both Crown Estate maximum capacity limitation per zone and a maximum number of wind turbines that can be placed in each zone's sites were considered as constraints in the optimisation problem. These were selected because of the possibility that the constraints might overlap in an extreme case scenario. Therefore, both constraints were added to the problem in order to secure all cases.

Table 4
Maximum capacity of Round 3 wind farms, specified by the Crown estate.

Zone	Capacity MW
1. Moray Firth	1500
2. Firth of Forth	3465
3. Dogger Bank	9000
4. Hornsea	4000
5. East Anglia	7200
6. Rampion	665
7. Navitas| Bay	1200
8. Bristol Channel	1500
9. Celtic Array	4185
TOTAL CAPACITY	32715

For the estimation of cabling length, which is required to calculate parts of the LCC related to the spatial distribution of the wind turbines in the wind farm, the minimum spanning tree algorithm is used. The location of the turbines is treated as a set of vertices of a graph and the cabling represents the edges that connect the vertices. Given a set of vertices, which are separated by each other by the different layout indices, from Fig. 6, the minimum spanning tree connects all these vertices without creating any cycles, thus yielding minimum possible total edge length. This represents the minimum cable length of the particular layout.

The whole framework has been implemented by using Python 3. The optimisation modelling has been completed using the library platypus in python [54] and the sensitivity analysis using the method Sobol Indices [55] by using the library SALib [56].

Also, the physical features of the site cannot allow turbine installation in all parts of the seabed. Also, the assumption that the offshore sites can host up to a maximum number of turbines was introduced without considering any site investigations or initial capital cost.

4. Results and discussion

The LCC model described in the methodology was used in the optimisation problem and 8 objectives were included in the process by utilising the NSGA II algorithm according to Fig. 1. The outcomes show trade-offs between important factors such as CAPEX vs OPEX and the total costs for each solution individually. By applying the framework described above, the optimal recommendations for deploying an offshore wind farm are produced. First, the available sites are selected along with the specifications of each site. Also, a range of wind turbines is selected along with their specifications. Both of the above are used as an input to the LCC. Next, the configuration settings of the optimisation function are specified and the optimisation algorithm runs by utilising the aforementioned LCC.

First, the results from all locations (from all five zones) are provided and illustrated in Figs. 8 and 9, accordingly. Second, the results for each zone individually are provided and illustrated below from Figs. 10–14. Each case includes the results from all layouts for comparison. A new simulation was performed for each zone, from scratch; a zone can include for example 2 locations (Moray Firth Zone), 6 locations (East Anglia Zone), etc. All results shown and discussed are equally optimal solutions, according to the Pareto equality.

4.1. Location selection for all layouts for 18 locations (5 round 3 zones)

Here, the results include all 18 locations acquired from the five selected Round 3 zones. The comparison includes CAPEX versus OPEX costs and total costs, as shown in Figs. 8 and 9. Overall, for all layouts, the solutions from the trade-off according to CAPEX and OPEX are shown in Fig. 8. All layouts were found to deliver optimal solutions, where the 10–18 layout was found only once with few turbines. In the range between £1.6 and £1.8 billion of total cost, 4 solutions were discovered, for the areas of Seagreen Alpha, East Anglia One and Hornsea Project One.

The breakdown of all costs is depicted in Fig. 9 by normalising the total cost per MW of installed capacity (throughout the lifecycle of the project). Norfolk Boreas seems to include the highest total costs per MW compared to the rest of the sites. The gap between the highest and lowest cost solutions is approximately £2 million per MW. On average, CAPEX per MW is ten times larger than OPEX per MW, while OPEX per MW and $C_{D\&D}$ per MW are comparable in size.

4.2. Location selection for all layouts per round 3 zone

Here, the same methodology was applied to each zone individually from the five selected Round 3 zones, the trade-offs

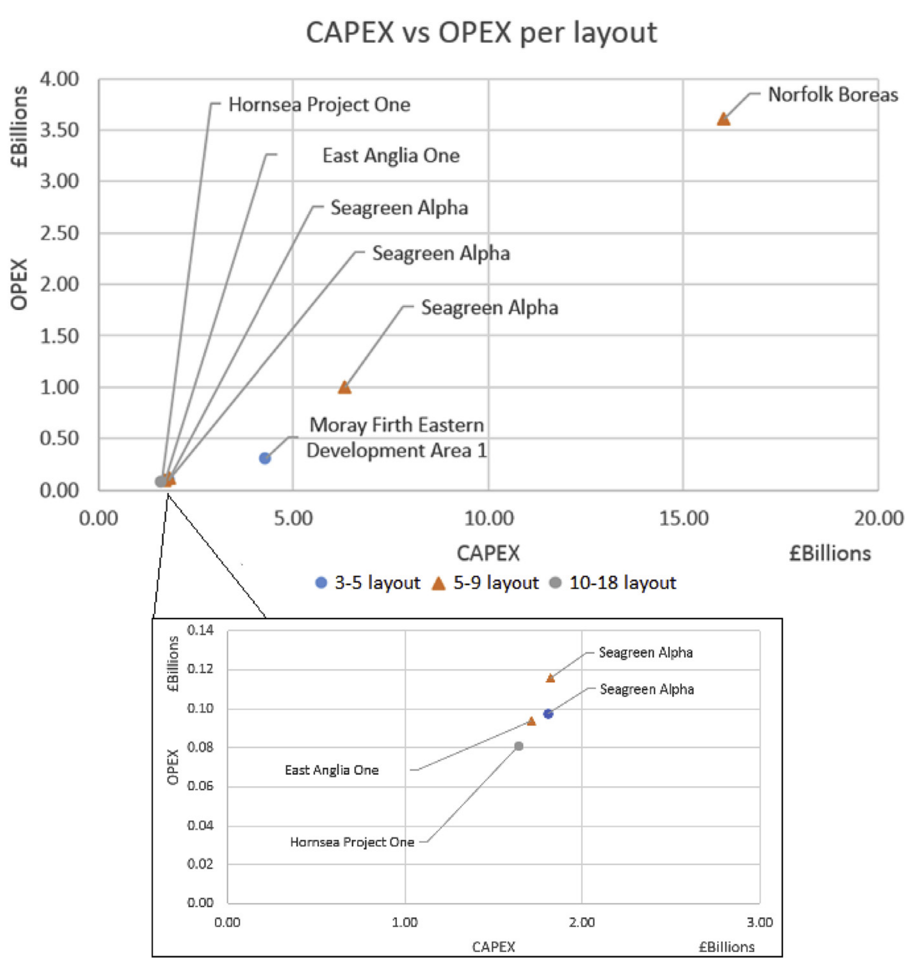

Fig. 8. OPEX vs CAPEX for all PF solutions for all layout cases and solutions focused on the beginning of the trend of the costs.

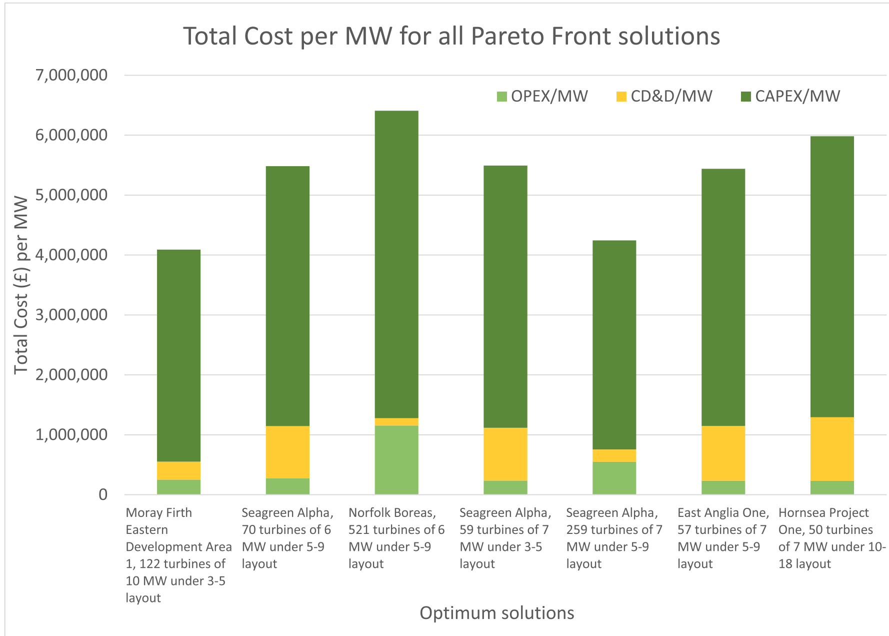

Fig. 9. Total Cost per MW for all Pareto Front solutions.

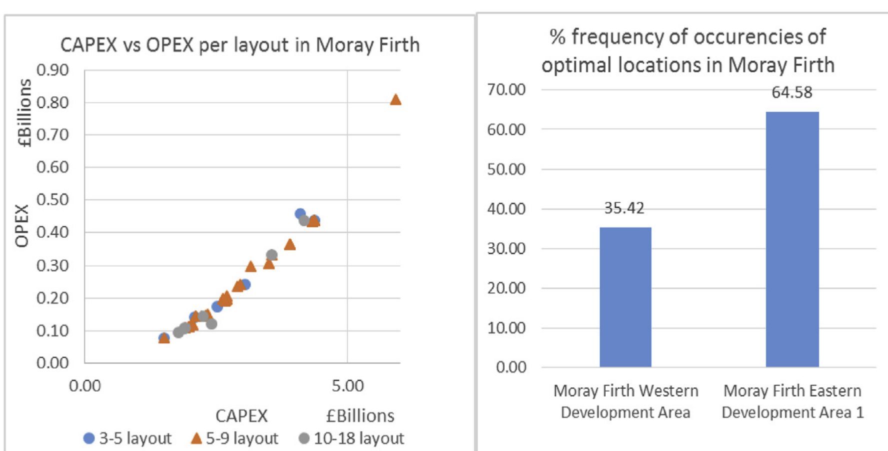

Fig. 10. (a) Comparing OPEX vs CAPEX for the zone of Moray Firth for all layout cases and (b) % of frequency in the PF front for the zone of Moray Firth and all layout cases.

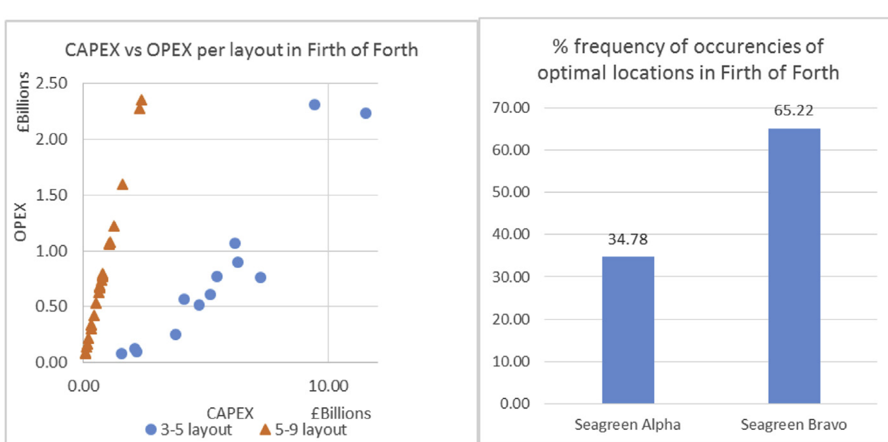

Fig. 11. (a) Comparing OPEX vs CAPEX for the zone of Firth of Forth for all layout cases and (b) % of frequency in the PF for the zone of Firth of Forth and all layout cases.

between CAPEX and OPEX and the relative frequency in the PF solutions are shown from Figs. 10–14.

For Moray Firth, the trade-off between CAPEX vs OPEX appears more concentrated, as shown in Fig. 10(a) where CAPEX and OPEX vary together irrespectively of the considered layouts, which suggests that the sites present a similar performance for different layouts. In one extreme case, the 5–9 layout is far from the cluster of points. The revealed solutions for this zone present the lowest costs in terms of CAPEX and OPEX. In the aggregated frequency, in Fig. 10(b), in Moray Firth, Moray Firth Eastern Development 1, the gap appears almost twice as much as Moray Firth Western Development Area.

The solutions of Firth of Forth follow different trends per layout in the CAPEX vs OPEX trade-off, in Fig. 11(a), where it is also shown that for the 3–5 layout, OPEX develops much faster than CAPEX as the costs increase. The opposite holds for 5–9 layout. The clear separation of layouts, where the performance of CAPEX vs OPEX for 5–9 layout seems to vary linearly, which indicates that the choice of layout is more important in Firth of Forth compared to all other cases. The 10–18 layout was not found in this case. In the frequencies, the optimum results Seagreen Bravo appears almost twice as much as Seagreen Alpha in Fig. 11(b).

The detailed analysis for Dogger Bank is similar to the analysis for all the regions, performed in the above section. As shown in Fig. 12(a), only 3–5 and 5–9 layouts were selected and three solutions from 3 to 5 layout appear at the bottom left corner. This site is the most expensive in terms of CAPEX and OPEX. Then, in Fig. 12(b), Creyke Beck B gathered the highest percentage of non-dominated solutions. Also, Teeside C, Teeside D and Tranche and 10–18 layout were not selected by the optimiser in this case.

The 5–9 layout seems to be the most frequent in Hornsea, as shown in Fig. 13(a). A few solutions from 10 to 18 layout appear at the bottom left corner and there is a discontinuity in the optimal results, which proves the ability of the optimiser to reveal solutions in a small region of optimal performance and distant regions. Fig. 13(b), Hornsea Project Three and Four present similar frequencies. Hornsea Project Two was not selected by the optimiser.

In East Anglia, most optimal solutions are of 3–5 layout, as shown in Fig. 14(a). Relative to the other cases, the percentages of frequency demonstrate little discrepancy, as shown in Fig. 14(b) which means that all of them can be selected by developers. 10–18 layout was not selected by the optimiser. The discontinuity in the results for 3–5 layout between approximately £12 billion and £30 billion in CAPEX demonstrates the gap in the attainable trade-off.

Regarding the frequency of revealed solutions, one can notice 3 clusters. The first cluster, in terms of highest percentage, includes two areas that were equally visited by the NSGAII. The second cluster comprises of three areas that were visited by 13.33%. The last cluster includes a single location, which had been visited half of the times of the previous cluster.

4.3. Sensitivity analysis

For the purposes of the sensitivity analysis, the levels of 80, 100, 120, 150 were utilised for population size and 2, 3, 4, 5 were utilised for the tournament selection of the algorithm. The quality of the discovered trade-offs was assessed by employing the hypervolume indicator of the points in the trade-off as shown in Ref. [57] (also provided by platypus library), where the reference point was a high dimensional point from the trade-off with the most extreme and dominated value for each component of the reference point. Each combination of population size and tournament selection was executed for ten times and the respective variance was calculated for each set, whose results are listed in Table 5.

The results of the hypervolume calculation varied between the order of magnitude of 10^{57} and 10^{59}. According to this range, the value of variance is consistently negligible, which suggests that the selection of the aforementioned settings for NSGA II does not impact on the operation of the algorithm and its ability to reveal an optimal trade-off. The results of this study, presented in Subsections 4.1 and 4.2, were produced by using the population size of 100 and tournament selection of 2, based on authors' experience.

Following the dissimilarities in the trade-off of the cases analysed above, a sensitivity analysis has been performed to further investigate the diverse behaviour. The overall sensitivity of decision variables and their pairwise sensitivity are depicted in Figs. 15 and 16, respectively, by calculating Sobol indices. In a sensitivity analysis, Sobol indices explain the importance of an input factor on the variance of the output. Consequently, ST, S1 and S2 correspond to total order sensitivity index, first order and second order sensitivity index (i.e. corresponds to pairwise sensitivities between variables), respectively.

According to Fig. 15, all variables have high ST index. Here, the categorical variables are treated as integers. Hence, the absolute value will be considered for this sensitivity analysis. The confidence interval for S1 is less than 10%, which shows that the sample size is sufficient to deduct conclusions and the absolute value of S1 is too

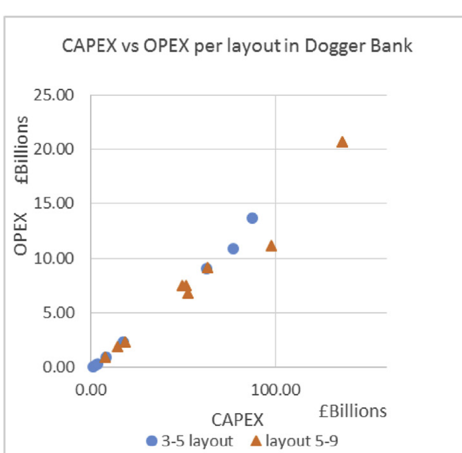

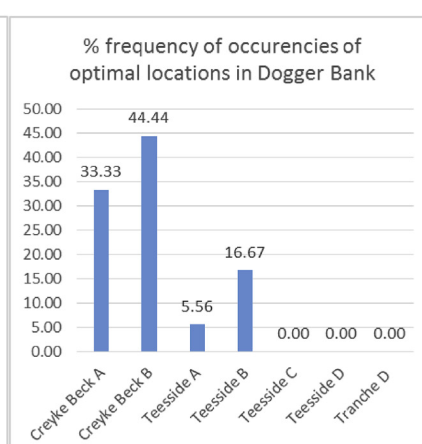

Fig. 12. (a) Comparing OPEX vs CAPEX for the zone of Dogger Bank for layout case 1 and 2 and (b) % of frequency in the PF for the zone of Dogger Bank and both layout cases 1 and 2.

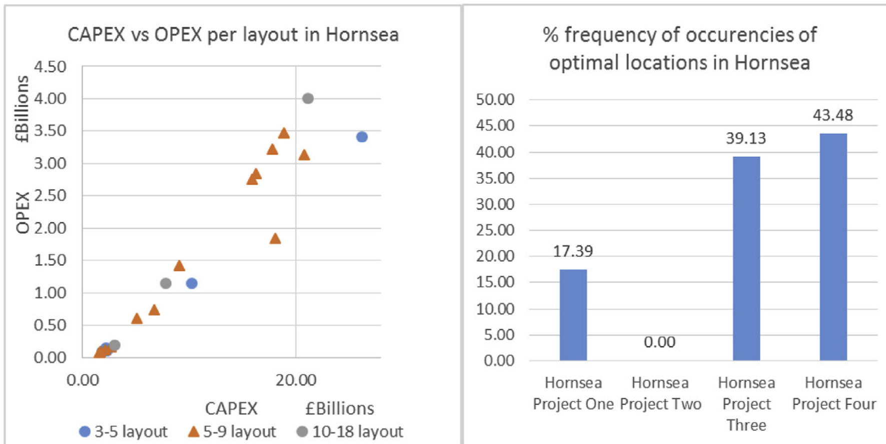

Fig. 13. (a) Comparing OPEX vs CAPEX for the zone of Hornsea for all layout cases and (b) % of frequency in the PF front for the zone of Hornsea and all layout cases.

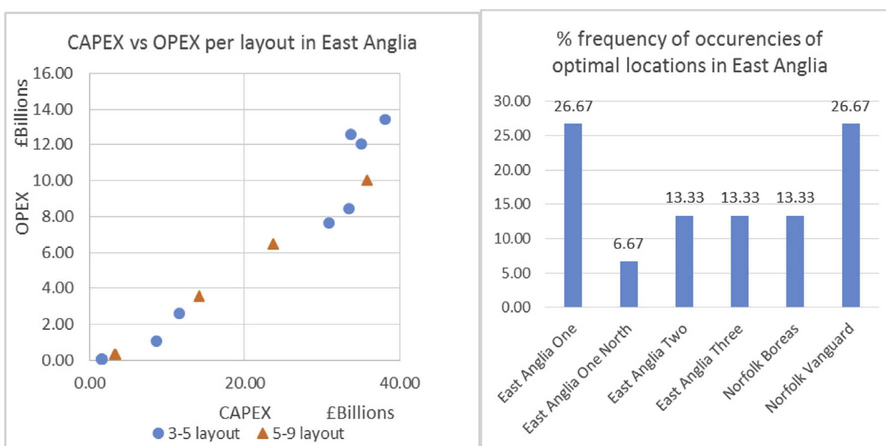

Fig. 14. (a) Comparing OPEX vs CAPEX for the zone of East Anglia for all layout cases and (b) % of frequency in the PF front for the zone of East Anglia and all layout cases.

Table 5
Variance of hypervolume indicator, through statistical sensitivity analysis, by altering the configuration parameters of NSGA II.

Population size	Tournament			
	2	3	4	5
80	1.172723	1.345013	0.988865	1.40078
100	0.955844	0.975384	0.976562	1.451503
120	1.070043	1.109467	0.94458	0.826054
150	0.734528	1.031415	0.979032	1.138782
200	0.63721	1.013199	0.714002	0.861545

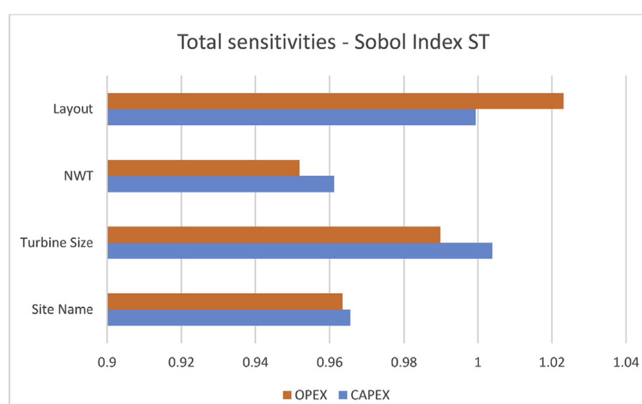

Fig. 15. Total sensitivity based on Sobol indices.

low, which means that varying a single variable at a time has little impact on CAPEX and OPEX. S2 in Fig. 16 provides deeper insight and verifies the complexity of the problem. For the S2 index, more samples are required to accurately identify the interactions among the variables. The combination of the site and the layout is the most powerful pair to cause a change both for CAPEX and OPEX. Then, the site and the turbine size is the second most powerful combination to cause a change to both CAPEX and OPEX.

It is important to note that the sample size for the current modelling in the framework has more than 20,000 samples, which has captured a fraction of the total sensitivity. The investigation of higher orders of Sobol indices could be explored in the future, so as to reveal the importance of the combination of more inputs. Negative sensitivities shown in Fig. 16 could be addressed by acquiring additional samples. Hence, it is expected that the combination of multiple input changes at the same time could more

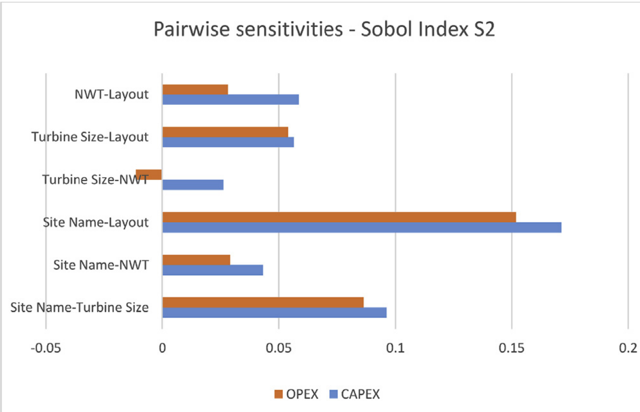

Fig. 16. Pairwise sensitivity.

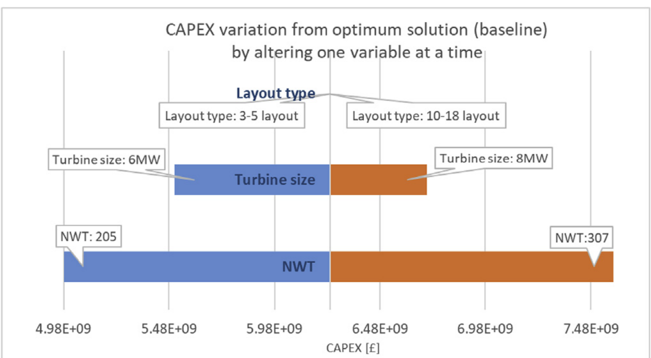

Fig. 17. CAPEX variation from optimum solution (baseline) by altering one variable at a time.

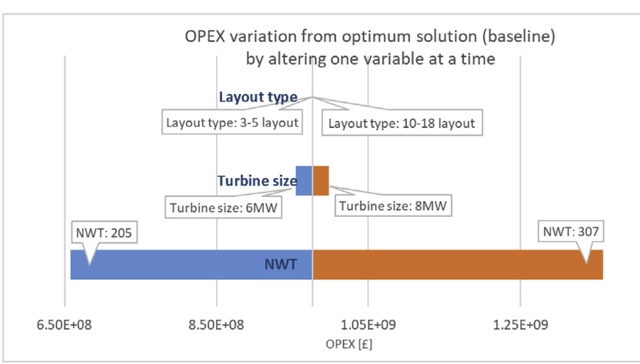

Fig. 18. OPEX variation from optimum solution (baseline) by altering one variable at a time.

drastically affect CAPEX, OPEX and the remaining objectives. Potentially, changing the modelling could consider a wider range of inputs to provide a deeper insight into the original problem, but this would increase the computational cost.

In order to illustrate the above abstract observation, a demonstration of the sensitivity of the problem is provided below. More specifically, a reference case was selected among the optimum solutions revealed above for which the decision variables changed one at a time. The solution that was chosen is in Seagreen Alpha under 5–9 layout with 259 turbines of 7 MW. By considering the previous solution as the baseline, the number of turbines varied by 20% (±20%), the layout type changed to 3–5 layout and 10–18 layout, and finally the turbine type changed to 6 MW and 8 MW, as shown in Figs. 17 and 18, for CAPEX and OPEX, respectively. Clearly, the number of turbines causes the greatest change, whereas a change in the layout yields such a little change that is very hard to notice.

5. Conclusion

This study demonstrated the effectiveness of a methodology by linking MOO with LCC as objective functions and comparing three different wind farm layouts in order to select the optimum solutions. The results provided greater insight into the decision-making process to develop an offshore wind farm through optimisation techniques by considering different wind turbine layouts, number of turbines, Round 3 locations in the UK and turbine size.

Trade-offs between the CAPEX and OPEX were revealed and further investigated by conducting a sensitivity analysis. When optimising all the regions together, in the range between 1.6 and 1.8 billion, four optimum solutions were discovered, for the areas of Seagreen Alpha, East Anglia One and Hornsea Project One. Although 3–5 and 5–9 layouts were mainly selected as optimum solutions by the optimiser, 10–18 layout (i.e., the extreme case) also appeared in the PF solutions a few times. When optimising 5 zones separately, Moray Firth Eastern Development area 1 was mostly chosen in Moray Firth and Seagreen Bravo in Firth of Forth. The results of optimisation in East Anglia were the most balanced, which recommend that all sites are equally appropriate to be selected. In Hornsea, Hornsea Project Two was never selected in the PF. In Dogger Bank, Creyke A and B amount for 77% of the optimum solutions, whereas Teeside C and D, and Tranche D were never selected. The sensitivity analysis demonstrated the highly complex nature of the decision variables and their interdependencies, where the combinations of site-layout and site-turbine size captured above 20% of the variability in CAPEX and OPEX. Higher-order interdependencies will be investigated in the future.

The revealed outcomes will have an important impact on a possible extension of the Round 3 zones in the future of the UK and will help decision makers for their next cost-efficient investment decision. The proposed framework could also be applied to other sectors in order to increase investment confidence and reveal optimum solutions. For example, the framework can be applied to the installation of floating offshore wind and wave devices, where the optimum locations can be suggested according to cost and operational aspects of each technological need.

Acknowledgements

This work was supported by Grant EP/L016303/1 for Cranfield University, Centre for Doctoral Training in Renewable Energy Marine Structures (REMS) (http://www.rems-cdt.ac.uk/) from the UK Engineering and Physical Sciences Research Council (EPSRC). Data underlying this paper can be accessed at https://doi.org/10.17862/cranfield.rd.6551396.

Appendix A

Table 6
Maximum number of turbines for each offshore site employing 10 MW turbines and 3 layout cases.

Zone	Wind farm site name	Area (km^2)	Max Number of turbines (3–5 layout, X = 3D, Y = 5D)	Max Number of turbines (5–9 layout, X = 5D, Y = 9D)	Max Number of turbines (10–18 layout, X = 10D, Y = 18D)
Moray Firth	Moray Firth Western Development Area	226	1487	492	125
Moray Firth	Moray Firth Eastern Development Area 1	295	1957	652	164
Firth of Forth	Seagreen Alpha	197	1211	404	97
Firth of Forth	Seagreen Bravo	194	1161	387	97
Dogger Bank	Creyke Beck A	515	2850	949	238
Dogger Bank	Creyke Beck B	599	3345	1119	281
Dogger Bank	Teesside A	562	3137	1047	261
Dogger Bank	Teesside B	593	3309	1079	265
Hornsea	Hornsea Project One	407	1533	510	181
Hornsea	Hornsea Project Two	483	3058	1022	204
Hornsea	Hornsea Project Three	3875	3683	1226	308
Hornsea	Hornsea Project Four	3874	4520	1502	380
East Anglia (Norfolk Bank)	East Anglia One	297	1010	340	86
East Anglia (Norfolk Bank)	East Anglia One North	206	1024	340	87
East Anglia (Norfolk Bank)	East Anglia Two	358	1242	416	105
East Anglia (Norfolk Bank)	East Anglia Three	301	3028	1014	128
East Anglia (Norfolk Bank)	Norfolk Boreas	727	3571	1226	308
East Anglia (Norfolk Bank)	Norfolk Vanguard	574	1493	497	249

Table 7
Maximum number of turbines for each offshore site employing 8 MW turbines and 3 layout cases.

Zone	Wind farm site name	Area (km^2)	Max Number of turbines (3–5 layout, X = 3D, Y = 5D)	Max Number of turbines (5–9 layout, X = 5D, Y = 9D)	Max Number of turbines (10–18 layout, X = 10D, Y = 18D)
Moray Firth	Moray Firth Western Development Area	226	1996	665	167
Moray Firth	Moray Firth Eastern Development Area 1	295	2618	876	219
Firth of Forth	Seagreen Alpha	197	1619	539	133
Firth of Forth	Seagreen Bravo	194	1566	525	131
Dogger Bank	Creyke Beck A	515	3820	1268	320
Dogger Bank	Creyke Beck B	599	4492	1491	378
Dogger Bank	Teesside A	562	4211	1401	349
Dogger Bank	Teesside B	593	4455	1483	358
Hornsea	Hornsea Project One	407	2058	683	242
Hornsea	Hornsea Project Two	483	4108	1369	276
Hornsea	Hornsea Project Three	3875	4946	1650	412
Hornsea	Hornsea Project Four	3874	6066	2024	502
East Anglia (Norfolk Bank)	East Anglia One	297	1357	452	111
East Anglia (Norfolk Bank)	East Anglia One North	206	1378	462	114
East Anglia (Norfolk Bank)	East Anglia Two	358	1680	558	140
East Anglia (Norfolk Bank)	East Anglia Three	301	4068	1355	169
East Anglia (Norfolk Bank)	Norfolk Boreas	727	4891	1655	413
East Anglia (Norfolk Bank)	Norfolk Vanguard	574	2000	669	337

Table 8
Maximum number of turbines for each offshore site employing 7 MW turbines and 3 layout cases.

Zone	Wind farm site name	Area (km^2)	Max Number of turbines (3–5 layout, X = 3D, Y = 5D)	Max Number of turbines (5–9 layout, X = 5D, Y = 9D)	Max Number of turbines (10–18 layout, X = 10D, Y = 18D)
Moray Firth	Moray Firth Western Development Area	226	2262	758	188
Moray Firth	Moray Firth Eastern Development Area 1	295	2974	988	247
Firth of Forth	Seagreen Alpha	197	1839	613	150
Firth of Forth	Seagreen Bravo	194	1775	588	151
Dogger Bank	Creyke Beck A	515	4333	1449	362
Dogger Bank	Creyke Beck B	599	5089	1693	428
Dogger Bank	Teesside A	562	4774	1591	398
Dogger Bank	Teesside B	593	5051	1691	411
Hornsea	Hornsea Project One	407	2332	777	269
Hornsea	Hornsea Project Two	483	4687	1552	315
Hornsea	Hornsea Project Three	3875	5607	1875	468
Hornsea	Hornsea Project Four	3874	6878	2294	576
East Anglia (Norfolk Bank)	East Anglia One	297	1538	1538	126
East Anglia (Norfolk Bank)	East Anglia One North	206	1562	1562	129
East Anglia (Norfolk Bank)	East Anglia Two	358	1899	633	159
East Anglia (Norfolk Bank)	East Anglia Three	301	4612	4612	197
East Anglia (Norfolk Bank)	Norfolk Boreas	727	5620	1878	462
East Anglia (Norfolk Bank)	Norfolk Vanguard	574	2269	756	376

Table 9
Maximum number of turbines for each offshore site employing 6 MW turbines and 3 layout cases.

Zone	Wind farm site name	Area (km^2)	Max Number of turbines (3–5 layout, X = 3D, Y = 5D)	Max Number of turbines (5–9 layout, X = 5D, Y = 9D)	Max Number of turbines (10–18 layout, X = 10D, Y = 18D)
Moray Firth	Moray Firth Western Development Area	226	2737	914	227
Moray Firth	Moray Firth Eastern Development Area 1	295	3596	1197	299
Firth of Forth	Seagreen Alpha	197	2229	741	182
Firth of Forth	Seagreen Bravo	194	2146	716	184
Dogger Bank	Creyke Beck A	515	5241	1746	438
Dogger Bank	Creyke Beck B	599	6157	2059	513
Dogger Bank	Teesside A	562	5777	1926	480
Dogger Bank	Teesside B	593	6118	2053	521
Hornsea	Hornsea Project One	407	2815	935	332
Hornsea	Hornsea Project Two	483	5643	1881	376
Hornsea	Hornsea Project Three	3875	6783	2257	568
Hornsea	Hornsea Project Four	3874	8326	2777	691
East Anglia (Norfolk Bank)	East Anglia One	297	1860	617	154
East Anglia (Norfolk Bank)	East Anglia One North	206	1894	627	157
East Anglia (Norfolk Bank)	East Anglia Two	358	2303	764	192
East Anglia (Norfolk Bank)	East Anglia Three	301	5579	1862	234
East Anglia (Norfolk Bank)	Norfolk Boreas	727	6799	2271	564
East Anglia (Norfolk Bank)	Norfolk Vanguard	574	2745	916	460

References

[1] BEC CREW. Here's what you need to know about the new paris climate deal. http://www.sciencealert.com/here-s-what-you-need-to-know-about-the-climate-deal-from-paris Accessed 2017.
[2] Department of Energy and Climate Change, Uk renewable Energy Roadmap, 2011.
[3] Global Wind Energy Council. Wind in numbers. http://www.gwec.net/global-figures/wind-in-numbers/[Access 2017].
[4] RenewableUK. Wind energy statistics. http://www.renewableuk.com/page/UKWEDhome Accessed 2018.
[5] V. Mytilinou, A.J. Kolios, G. Di Lorenzo, A comparative multi-disciplinary policy review in wind energy developments in europe, Int. J. Sustain. Energy (2015) 1–21.
[6] European Observation Network for Territorial Development and Cohesion. Inspire policy making by territorial evidence. http://www.espon.eu/main/Menu_Publications/Menu_MapsOfTheMonth/map1101.html Accessed 2017.
[7] S.-Y. Lin, J.-F. Chen, Distributed optimal power flow for smart grid transmission system with renewable energy sources, Energy 56 (2013) 184–192.
[8] Renewables First. What are the main project risks for wind power? https://www.renewablesfirst.co.uk/windpower/windpower-learning-centre/what-are-the-main-project-risks-for-wind-power/Accessed 2017.
[9] HM Government, Offshore Wind Industrial Strategy Business and Government

Action, 2013.
[10] V. Mytilinou, A.J. Kolios, A multi-objective optimisation approach applied to offshore wind farm location selection, J. Ocean Eng. Marine Energy (2017) 1–20.
[11] T. Burton, N. Jenkins, D. Sharpe, E. Bossanyi, Wind Energy Handbook, second ed., Wiley, 2011.
[12] The Crown Estate, Round 3 Zone Appraisal and Planning, A strategic approach to zone design, project identification and consent, 2010.
[13] The Crown Estate. The crown estate announces round 3 offshore wind development partners. http://www.thecrownestate.co.uk/news-and-media/news/2010/the-crown-estate-announces-round-3-offshore-wind-development-partners/Accessed 2017.
[14] The Crown Estate, Round 3 Offshore Wind Site Selection at National and Project Levels, 2013.
[15] D. Floor, Round 3 Offshore Wind Farms uk Future Energy Scenarios Seminar 2012, FOREWIND, 2012.
[16] D.F. Jones, G. Wall, An extended goal programming model for site selection in the offshore wind farm sector, Ann. Oper. Res. 245 (1-2) (2015) 121–135.
[17] L. Cradden, C. Kalogeri, I.M. Barrios, G. Galanis, D. Ingram, G. Kallos, Multi-criteria site selection for offshore renewable energy platforms, Renew. Energy 87 (Part 1) (2016) 791–806.
[18] A. Arias-Rosales, G. Osorio-Gómez, Wind turbine selection method based on the statistical analysis of nominal specifications for estimating the cost of energy, Appl. Energy 228 (2018) 980–998.
[19] Z. Bian, Z. Xu, L. Xiao, H. Dong, Q. Xu, Selection of optimal access point for offshore wind farm based on multi-objective decision making, Int. J. Electr. Power Energy Syst. 103 (2018) 43–49.
[20] S.K. Fuller, S.R. Petersen, Life-cycle Costing Manual for the Federal Energy Management Program, NIST handbook 1996, edition, 1995, p. 135.
[21] M. Nordahl, The Development of a Life Cycle Cost Model for an Offshore Wind Farm, Chalmers University of Technology, Göteborg, Sweden, 2011.
[22] N. Jungbluth, C. Bauer, R. Dones, R. Frischknecht, Life cycle assessment for emerging technologies: case studies for photovoltaic and wind power (11 pp), Int. J. Life Cycle Assess. 10 (2005) 24–34.
[23] L. Schleisner, Life cycle assessment of a wind farm and related externalities, Renew. Energy 20 (2000) 279–288.
[24] J. Nilsson, L. Bertling, Maintenance management of wind power systems using condition monitoring systems—life cycle cost analysis for two case studies, IEEE Trans. Energy Convers. 22 (2007) 223–229.
[25] A. Myhr, C. Bjerkseter, A. Ågotnes, T.A. Nygaard, Levelised cost of energy for offshore floating wind turbines in a life cycle perspective, Renew. Energy 66 (2014) 714–728.
[26] C.-S. Laura, D.-C. Vicente, Life-cycle cost analysis of floating offshore wind farms, Renew. Energy 66 (2014) 41–48.
[27] E. Martínez, F. Sanz, S. Pellegrini, E. Jiménez, J. Blanco, Life cycle assessment of a multi-megawatt wind turbine, Renew. Energy 34 (2009) 667–673.
[28] K. Angelakoglou, P.N. Botsaris, G. Gaidajis, Issues regarding wind turbines positioning: a benchmark study with the application of the life cycle assessment approach, Sustain. Energy Technol. Assessments 5 (2014) 7–18.
[29] M. Shafiee, F. Brennan, I.A. Espinosa, Whole life-cycle costing of large-scale offshore wind farms, in: Conference: European Wind Energy Association (EWEA), EWEA, Paris, France, 2015.
[30] Y. Yuan, H. Xu, B. Wang, An improved nsga-iii procedure for evolutionary many-objective optimization, in: Proceedings of the 2014 Annual Conference on Genetic and Evolutionary Computation, ACM, 2014, pp. 661–668.
[31] B. Saavedra-Moreno, S. Salcedo-Sanz, A. Paniagua-Tineo, L. Prieto, A. Portilla-Figueras, Seeding evolutionary algorithms with heuristics for optimal wind turbines positioning in wind farms, Renew. Energy 36 (2011) 2838–2844.
[32] C.N. Elkinton, J.F. Manwell, J.G. McGowan, Algorithms for offshore wind farm layout optimization, Wind Eng. 32 (2008) 67–84.
[33] C. Wan, J. Wang, G. Yang, H. Gu, X. Zhang, Wind farm micro-siting by Gaussian particle swarm optimization with local search strategy, Renew. Energy 48 (2012) 276–286.
[34] J.S. González, A.G. Gonzalez Rodriguez, J.C. Mora, J.R. Santos, M.B. Payan, Optimization of wind farm turbines layout using an evolutive algorithm, Renew. Energy 35 (2010) 1671–1681.
[35] E. Papatheou, N. Dervilis, A.E. Maguire, I. Antoniadou, K. Worden, A performance monitoring approach for the novel lillgrund offshore wind farm, IEEE Trans. Ind. Electron. 62 (2015) 6636–6644.
[36] G. Yan, Research on Green Suppliers' Evaluation Based on Ahp & Genetic Algorithm, International Conference on Signal Processing Systems, 2009, pp. 615–619.
[37] M. Karimi, M. Hall, B. Buckham, C. Crawford, A multi-objective design optimization approach for floating offshore wind turbine support structures, J. Ocean Eng. Marine Energy 3 (2017) 69–87.
[38] C.N. Elkinton, J.F. Manwell, J.G. McGowan, Optimizing the layout of offshore wind energy systems, Mar. Technol. Soc. J. 42 (2008) 19–27.
[39] M. Samorani, The wind farm layout optimization problem, in: P.M. Pardalos, S. Rebennack, M.V.F. Pereira, N.A. Iliadis, V. Pappu (Eds.), Handbook of Wind Power Systems, Springer Berlin Heidelberg, Berlin, Heidelberg, 2013, pp. 21–38.
[40] C. Elkinton, J. Manwell, J. McGowan, Offshore wind farm layout optimization (owflo) project: preliminary results, in: 44th Aiaa Aerospace Sciences Meeting and Exhibit, American Institute of Aeronautics and Astronautics, 2006.
[41] L.J. Vermeer, J.N. Sørensen, A. Crespo, Wind turbine wake aerodynamics, Prog. Aero. Sci. 39 (2003) 467–510.
[42] G. Mosetti, C. Poloni, B. Diviacco, Optimization of wind turbine positioning in large windfarms by means of a genetic algorithm, J. Wind Eng. Ind. Aerod. 51 (1994) 105–116.
[43] N.O. Jensen, A Note on Wind Generator Interaction, Technical University of Denmark, 1983.
[44] Katic, I.; Højstrup, J.; Jensen, N.O. In A simple model for cluster efficiency, EWEC '86 1987; Palz, W.; Sesto, E., Eds. A. Raguzzi: pp 407-410.
[45] S. Şişbot, Ö. Turgut, M. Tunç, Ü. Çamdalı, Optimal positioning of wind turbines on gökçeada using multi-objective genetic algorithm, Wind Energy 13 (2010) 297–306.
[46] I.A. Espinosa, Life Cycle Costing of Offshore Wind Turbines Msc Thesis, Cranfield University, 2014.
[47] M. Dicorato, G. Forte, M. Pisani, M. Trovato, Guidelines for assessment of investment cost for offshore wind generation, Renew. Energy 36 (2011) 2043–2051.
[48] Wind energy The facts. Development and investment costs of offshore wind power. http://www.wind-energy-the-facts.org/development-and-investment-costs-of-offshore-wind-power.html Accessed 2017.
[49] 4COffshore. Global offshore wind farms database. http://www.4coffshore.com/offshorewind/index.html?lat=50.668&lon=-0.275&wfid=UK36 Accessed 2017.
[50] The Crown Estate, A Guide to an Offshore Wind Farm, The Crown Estate, 2017.
[51] QGIS. A free and open source geographic information system. http://www.qgis.org/en/site/index.html Accessed 2017.
[52] Fugro GEOS, Wind and Wave Frequency Distributions for Sites Around the British Isles, 2001.
[53] The Crown Estate. Maps and gis data. https://www.thecrownestate.co.uk/rural-and-coastal/coastal/downloads/maps-and-gis-data/Accessed 2017.
[54] Hadka, D. Platypus. http://platypus.readthedocs.io/en/latest/experimenter.html#comparing-algorithms-visually Accessed 2017.
[55] A. Saltelli, P. Annoni, I. Azzini, F. Campolongo, M. Ratto, S. Tarantola, Variance based sensitivity analysis of model output. Design and estimator for the total sensitivity index, Comput. Phys. Commun. 181 (2010) 259–270.
[56] J. Herman, W. Salib Usher, An open-source python library for sensitivity analysis, J. Open Source Software 2 (2017) 97.
[57] Y. Cao, B.J. Smucker, T.J. Robinson, On using the hypervolume indicator to compare pareto fronts: applications to multi-criteria optimal experimental design, J. Stat. Plann. Inference 160 (2015) 60–74.